

# MRI and $^{18}\text{F}$ FDG-PET in the assessment of bone marrow infiltration of the spine in cancer patients

Nadir Alexander Ghanem · Gregor Pache ·  
Christian Lohrmann · Ingo Brink · Thorsten Bley ·  
Elmar Kotter · Thomas Kelly · Mathias Langer

Received: 12 May 2006 / Revised: 8 February 2007 / Accepted: 22 February 2007 / Published online: 3 April 2007  
© Springer-Verlag 2007

**Abstract** The aim of this study was to evaluate the diagnostic value of MRI and  $^{18}\text{F}$ FDG-PET in bone marrow infiltration of the spine due to metastases of solid tumours and lymphoma in cancer patients. In 35 cancer patients (solid tumours  $n = 26$ , lymphoma  $n = 9$ ) MRI of the spine and  $^{18}\text{F}$ FDG-PET were reviewed and the detectability of metastases, infiltration of the spine, extent of disease, and therapeutic implications were compared. In 8/35 cases (23%) imaging technique showed concordantly no bone marrow infiltration. In 19/35 patients (54%), both MRI and  $^{18}\text{F}$ FDG-PET revealed bone marrow infiltration of the axial skeleton. In 12/19 patients (63%), MRI showed more extensive disease which lead to subsequent therapy. The imaging findings of MRI and  $^{18}\text{F}$ FDG-PET were discordant in 8/35 cases (23%).  $^{18}\text{F}$ FDG-PET was false positive in two patients. In six patients,  $^{18}\text{F}$ FDG-PET failed to detect bone metastases and bone marrow infiltration of the spine, which was detected by MRI and proven by clinical follow-up with subsequent therapy in two cases. MRI is more sensitive and specific than  $^{18}\text{F}$ FDG-PET detecting bone marrow metastases and infiltration of the spine and has a great impact in staging cancer patients.

**Keywords** Bone marrow infiltration · Spine · Lymphoma · Solid tumour · MRI ·  $^{18}\text{F}$ FDG-PET

## Introduction

The initial site of metastatic disease in bone is the bone marrow in patients with solid tumours with good prognosis [1]. Bone marrow involvement reveals a wide range in lymphoma patients, depending on the subclassification of lymphoma [4]. Early detection of bone marrow metastases and infiltration is crucial for tumour screening and staging to enable faster and accurate therapy and to decrease morbidity due to pain or complications [3–5]. Metastatic bone marrow involvement is found much more frequently (approximately 50–85%) at autopsy than in routine staging procedures [1].

The diagnosis of bone marrow metastasis and infiltration in cancer patients is most commonly addressed with bone scintigraphy, which has the advantage of generally high sensitivity and allowing a complete evaluation of the entire skeleton at relatively low cost [6, 20]. MRI may increase the sensitivity for detection of bone marrow involvement and bone marrow metastasis in patients with malignant lymphoma and solid tumours [2, 3, 5, 15]. There has been no previous study so far comparing  $^{18}\text{F}$ FDG-PET to MRI with respect to bone marrow infiltration caused by lymphoma and solid tumours, although both imaging techniques are well-established in daily clinical routine for cancer patients [7, 15].  $^{18}\text{F}$ FDG-PET is increasingly utilised for enquiries that had been reserved for skeletal scintigraphy, such as the detection of metastases and diagnosis of primary bone tumours [8–12]. Furthermore,  $^{18}\text{F}$ FDG-PET successfully administered the evaluation of musculoskeletal and intraosseous tumours and in detecting of osseous

N. A. Ghanem (✉) · G. Pache · C. Lohrmann ·  
T. Bley · E. Kotter · M. Langer  
Department of Diagnostic Radiology,  
University Hospital Freiburg, Hugstetter Strasse 55,  
79106 Freiburg, Germany  
e-mail: nadir.ghanem@uniklinik-freiburg.de

I. Brink · T. Kelly  
Department of Nuclear Medicine,  
University Hospital Freiburg, Freiburg, Germany

metastases of breast carcinoma and bone marrow involvement due to malignant lymphoma [8, 12, 14–17].

The purpose of this study was thus to evaluate the diagnostic value of  $^{18}\text{F}$ FDG-PET and MRI in detecting bone marrow infiltration of the spine in cancer patients.

## Materials and methods

### Patient population

A total of 35 cancer patients with various solid tumours ( $n = 26$ ) and lymphoma ( $n = 9$ ) underwent MRI examination of the spine to stage, follow-up known metastases or evaluate new bone pain or neurological symptoms.  $^{18}\text{F}$ FDG-PET was available in all these patients. Inclusion criterion was a timeframe of less than 1 month between  $^{18}\text{F}$ FDG-PET and MRI (mean 8.3 days, range 0–31 days, median 10.1 days).

Patients treated by chemotherapy or radiation therapy during the two examinations or 2 months prior to  $^{18}\text{F}$ FDG-PET, were excluded

The solid tumours consisted of the following: breast carcinoma  $n = 7$ , lung carcinoma  $n = 5$ , esophageal carcinoma  $n = 2$ , parotis carcinoma  $n = 2$ , hypopharynx carcinoma  $n = 2$ , cervical carcinoma  $n = 2$ , gastric carcinoma  $n = 1$ , pancreatic carcinoma  $n = 1$ , malignant melanoma  $n = 1$ , thyroid cancer  $n = 1$ , merkel-cell carcinoma  $n = 1$ , leiomyosarcoma  $n = 1$ . The lymphoma group consisted of: Non-Hodgkins lymphoma  $n = 5$ , Hodgkin lymphoma  $n = 3$ , plasmocytoma  $n = 1$ .

### Imaging

*Magnetic resonance imaging* was performed on high-field strength tomographs (1.5T) (Magnetom Symphony, Vision, Siemens Medical Solutions, Erlangen, Germany). Sagittal T1-W SE (TR 400–600 ms, TE 12–15 ms) and STIR sequence (TR 3,600–4,800 ms, TE 120 ms, TI 160 ms) were available with a matrix size of 256 or 512, rectangular field-of-view, number of acquisitions between 2 and 4, and a slice thickness between 4 and 6 mm.

Intravenous contrast media was used at a regular dosage of 0, 1 mmol Gd-DTPA (Magnevist, Schering, Berlin, Germany) per kg body weight in all cases. T1-weighted fat-suppressed spin echo sequences were performed following iv. contrast media application.

$^{18}\text{F}$ FDG-Positron emission tomography was performed as a routine staging procedure for the patient after referral by the clinician in charge. Patients fasted for at least 12 h prior to injection of the radiopharmaceutical to provide optimal conditions for tracer uptake. Blood glucose levels were

measured in all patients and did not exceed 110 mg/dl (6.1 mmol/l). After intravenous injection of  $360 \text{ MBq} \pm 30$  fluorine-18, deoxyglucose (FDG) emission scans were acquired 90 min later to optimise the tumour-to-background ratio. A two-dimensional ring scanner (Ecat Exact; Siemens/CTI, Knoxville, Tenn) equipped with a rod source for post-injection segmented attenuation correction was used. Eight to ten bed positions with an 11-cm transverse field of view were measured (2 min transmission and 8 min emission per position). Images were reconstructed by iteration with ordered subsets (ordered subset-expectation maximization, or OSEM, two iterations, eight subsets), no pre- or postfiltering was used, and final reconstruction resolution of the images was 6 mm. The reconstructed images were assessed on a computer monitor at all three levels in axial, coronal and sagittal views.

### Data analysis

#### *Magnetic resonance imaging*

Two radiologists (NG, CL) experienced in musculoskeletal imaging were blinded to both  $^{18}\text{F}$ FDG-PET findings and clinical results. They independently evaluated axial skeleton bone marrow in MRI. Again, disagreement was resolved by consensus reading in only two cases.

Criteria for a positive MRI finding were focal, multifocal or diffuse areas of decreased signal intensity in T1-W images with a relative increase in signal intensity in STIR sequences, and soft tissue tumours with continuity to bone marrow pathologies after exclusion of osteoporotic or traumatic fractures or spondylodiscitis. Focal areas of low signal in both images were interpreted as osteoblastic metastasis if there was a contrast media enhancement after iv. contrast media application.

#### *Positron emission tomography*

Two nuclear physicians (IB, TK) blinded to the MRI results read the PET scans independently and prospectively by consensus and determined the presence, extent, and location of metastases and marrow infiltration of the spine. Criteria for bone marrow infiltration and metastases in  $^{18}\text{F}$ FDG-PET were focal areas of increased tracer uptake or a diffusely increased uptake. Findings of extraspinal disease were excluded.

#### *Comparison of $^{18}\text{F}$ FDG-PET and MRI*

One or more of these bone marrows were investigated depending on the clinical indications: cervical spine ( $n = 7$ ), thoracic spine ( $n = 13$ ) or lumbar spine with sacral

bone ( $n = 15$ ). Only these anatomical regions were compared to  $^{18}\text{F}$ FDG-PET findings.

Patients with no lesions on PET and MRI exams were regarded as truly negative. Bone marrow infiltration or metastatic disease was assumed according to the criteria mentioned above in all cases of concordantly positive MRI and  $^{18}\text{F}$ FDG-PET findings. Discordant imaging results were resolved by clinical follow-up, comparison to CT or follow-up MRI,  $^{18}\text{F}$ FDG-PET and skeletal or bone marrow scintigraphy. Follow-up investigations were used to determine the true or false positive or the true or false negative nature of imaging findings in patients with discordant imaging results and for all discordant lesions. Further, in these patients with discordant extent of bone marrow infiltration and bone marrow metastases on  $^{18}\text{F}$ FDG-PET and MRI, a lesion-by-lesion analysis was performed in cases of progressive disease showing a lesion unequivocally increasing in size on follow-up.

Sensitivities, specificities and diagnostic accuracies were determined on a patient-by-patient basis. The evaluation focused on the presence and type (uni- or multifocal, or diffuse) infiltration pattern due to metastases or lymphoma, relative number of metastases compared to  $^{18}\text{F}$ FDG-PET, morphological criteria of affected vertebral bodies (fractures due to infiltration, involvement of posterior part of the vertebral body including the vertebral arcs and pedicles, spinal canal stenosis, spinal cord compression and paravertebral soft tissue tumors), as well as spinal cord metastases.  $^{18}\text{F}$ FDG-PET evaluation also included presence and frequency of bone marrow metastases and infiltration of the axial skeleton.

## Results

MRI and  $^{18}\text{F}$ FDG-PET findings in the spine were concordant in 27/35 patients (77%). In 8/35 cases (23%) MRI and  $^{18}\text{F}$ FDG-PET revealed no metastatic disease in solid tumours or bone marrow infiltration in lymphoma. In one of these eight patients with concordant negative imaging findings of the axial skeleton, MRI depicted a spinal cord metastasis of a lung carcinoma (Fig. 1). In another patient with a solid tumour, neither imaging technique revealed any bone marrow infiltration due to metastases, although MRI detected one intramedullary metastasis due to a Merkel cell tumor.

In 19/35 cancer patients (54%) MRI and  $^{18}\text{F}$ FDG-PET concordantly revealed bone marrow metastases and infiltration of the spine (Figs. 2, 3). In 12 of those 19 patients (63%) MRI showed more metastatic disease or bone marrow infiltration of the spine (Fig. 2). In seven cases of positive concordant imaging findings, the extent



**Fig. 1** A 60-year-old male with a lung carcinoma; time frame between MRI and  $^{18}\text{F}$ FDG-PET was 28 days. No previous therapy has been performed.  $^{18}\text{F}$ FDG-PET (a) shows no evidence of metastatic disease. In correlation with the  $^{18}\text{F}$ FDG-PET, MRI of the spine reveals no metastatic disease in the cervical spine. However, a solitary intramedullary metastasis is clearly seen on the T2-STIR weighted image (arrow) with subsequent therapy

of metastatic disease and bone marrow infiltration was similar described by MRI and  $^{18}\text{F}$ FDG-PET.

Yielding additional morphological information in 13/19 patients (68%) with concordant positive imaging findings MRI had a therapeutic impact in 7 of those 13 (54%).

MRI and  $^{18}\text{F}$ FDG-PET imaging findings were discordant in 8/35 cases (23%).  $^{18}\text{F}$ FDG-PET was false negative in six patients (lymphoma  $n = 4$ , solid tumors  $n = 2$ ) and failed to detect metastases and bone marrow infiltration later proven in MRI and the clinical follow up resulting in 2/6 cases in subsequent radiation therapy (Fig. 4). In two patients with lymphoma  $^{18}\text{F}$ FDG-PET was false positive, whereas the MRI of the spine demonstrated in both cases no evidence of bone marrow infiltration in either patient proven by clinical follow up. MRI was superior in six patients regarding the detection of bone marrow metastasis and infiltration due to solid tumors ( $n = 3$ ) and lymphoma ( $n = 3$ ).

MRI was positive, whereas  $^{18}\text{F}$ FDG-PET failed to detect bone marrow infiltration. MRI detected a multifocal bone marrow infiltration of the spine in three cases; all of those findings were proven in clinical follow-up and subsequent investigations (MRI  $n = 1$ , CT  $n = 1$ , skeletal scintigraphy  $n = 2$ , bone marrow scintigraphy  $n = 2$ ).

In three patients with lymphoma (Hodgkin lymphoma  $n = 1$ , NHL  $n = 2$ ), diffuse bone marrow infiltration was depicted by MRI, in one case in combination with a soft-tissue tumour. One of those patients underwent surgery due to neurological symptoms caused by a soft-tissue tumor.

**Fig. 2** A 60-year-old female with malignant melanoma. Time frame between MRI and  $^{18}\text{F}$ FDG-PET was only 4 days. **a**  $^{18}\text{F}$ FDG-PET reveals multifocal bone marrow involvement due to metastatic disease in the lumbar spine. **b** MRI demonstrates multifocal bone marrow infiltration due to metastatic disease in the lumbar spine and at level S1. (*left* T1-weighted image, *right* STIR image)

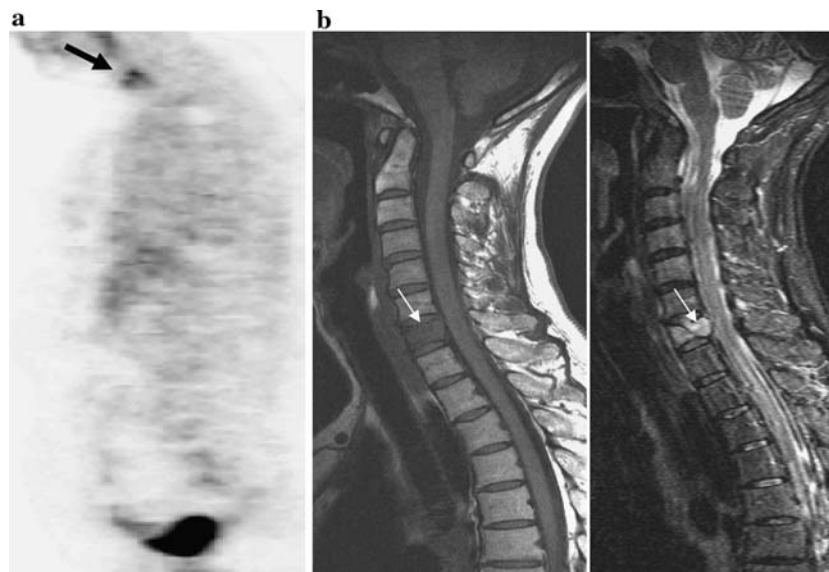
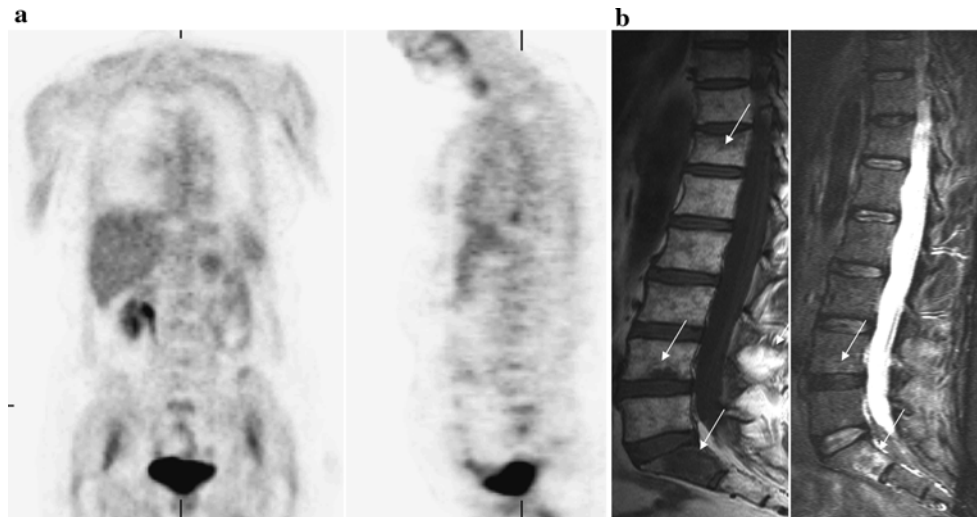


**Fig. 3** A 54-year-old female after surgery of a lung carcinoma. MRI and  $^{18}\text{F}$ FDG-PET were performed after skeletal scintigraphy revealed a solitary increased uptake of the cervical spine. **a** Concordantly with the bone scintigraphy,  $^{18}\text{F}$ FDG-PET reveals a solitary osseous metastasis in the cervical spine. **b** MRI demonstrates a diffuse

hypointense vertebra at level C7 on a T1-weighted image (*left side*) corresponding to a signal increase on the STIR sequence (*right side*). Note the small hypointense oblique line indicating a pathological fracture. There is a retropulsion of the posterior bony fragment into the spinal canal. This patient underwent subsequent radiation therapy

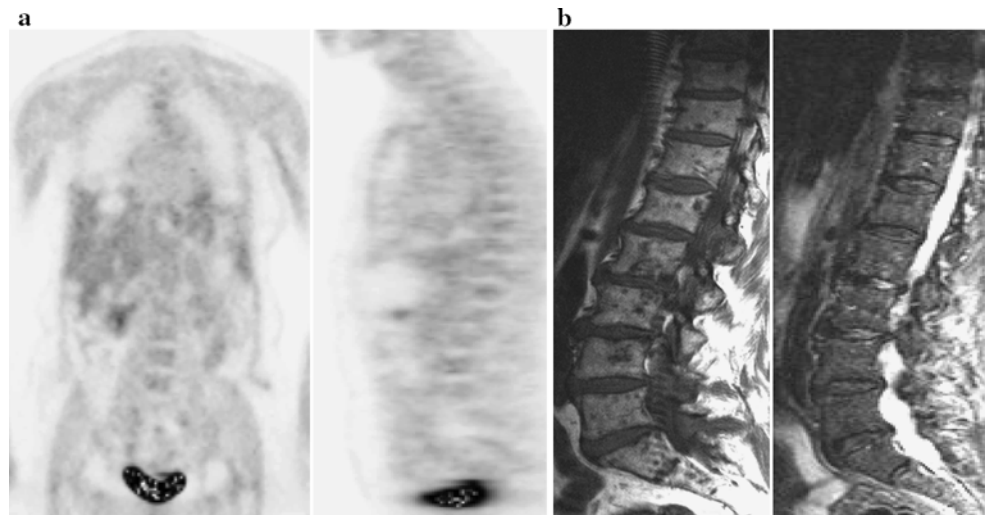
Three patients had discordant findings concerning bone marrow metastases from solid tumors. One of them suffered from lung carcinoma and two from breast carcinoma.

A diffuse bone marrow infiltration due to metastatic disease was observed in two of those three patients. A unifocal metastasis was seen in the third patient in combination with a medullary metastasis later proven in clinical follow-up.

MRI and  $^{18}\text{F}$ FDG-PET concordantly indicated the presence of bone marrow metastases and infiltration of

the spine in 19/35 (54%) patients. In 12 of those with positive concordant imaging findings (64%), MRI revealed the following additional morphological information: spinal canal stenosis ( $n = 8$ ), involvement of posterior parts of the vertebral body, including the vertebral arcs or pedicles ( $n = 9$ ), paravertebral and intraspinal soft tissue tumours ( $n = 7$ ), fractured vertebra ( $n = 1$ ), codfish vertebra ( $n = 2$ ) and spinal cord metastases ( $n = 1$ ). Local therapy was initiated in 7/12 patients [local radiation therapy ( $n = 6$ ), surgical treatment ( $n = 1$ )].

**Fig. 4** A 50-year-old female with breast cancer presenting with back pain. **a**  $^{18}\text{F}$ FDG-PET reveals no metastatic disease in the spine. In whole-body investigation, there was no relapse and no sign of distant metastases. **b** MRI shows a pathological bone marrow signal with a combined diffuse and multifocal infiltration pattern proven by a progressive metastatic disease. The metastases appear hypointense on T1-weighted images and exhibit a signal increase on T2-weighted STIR sequences (*right* T1-weighted image, *left* STIR sequence image)



Regarding bone marrow infiltration in lymphoma and solid tumor patients, MRI showed a disseminated pattern in 10/19 patients (53%), multifocal infiltration in 6/19 patients (32%), and unifocal metastases in 3/19 patients (16%). Conversely,  $^{18}\text{F}$ FDG-PET demonstrated a unifocal pattern in 6/19 (32%) patients, multifocal infiltration in 9/19 (47%) patients, and disseminated spine disease of the spine in 4/19 patients (21%).

## Discussion

First of all, we have to stress that bone marrow infiltration means a pre-radiological lesion due to metastatic or lymphoma disease, which can be only detected by MRI, PET (PET/CT) and bone marrow scintigraphy.

Few studies exist which directly compare MRI and  $^{18}\text{F}$ FDG-PET with respect to bone marrow metastases of solid tumours and bone marrow infiltration due to lymphoma [9, 14]. In contrast to previously published data, this study reveals MRIs greater sensitivity (78%), specificity (88%), and diagnostic accuracy (82%) than  $^{18}\text{F}$ FDG-PET in detecting bone marrow metastasis and infiltration in cancer patients.

Daldrup-Link et al. investigated 39 children and young adults with different tumour entities including sarcoma and lymphoma [9]. In detecting bone marrow metastasis and infiltration in cancer patients, they observed the following degrees of sensitivity: 90%  $^{18}\text{F}$ FDG-PET, 82% MRI and in 71% skeletal scintigraphy.  $^{18}\text{F}$ FDG-PET was demonstrated to be more sensitive than MRI and skeletal scintigraphy. When comparing  $^{18}\text{F}$ FDG-PET with bone scintigraphy, initial data suggest that  $^{18}\text{F}$ FDG-PET is more sensitive than conventional bone imaging [9, 13, 19]. However, some authors report that  $^{18}\text{F}$ FDG-PET is less sensitive than bone

scintigraphy in identifying osseous metastases, especially in prostate cancer and metastases of the osteosarcoma [12, 14].

Kao et al. investigated 24 patients with a biopsy-proven malignancy and suspected bone metastasis [14]. They found that  $^{18}\text{F}$ FDG-PET was negative in 11 metastatic and 20 benign bone lesions with a positive bone-scan finding. This indicates less sensitivity in detecting malignant bone metastases, but they concluded that  $^{18}\text{F}$ FDG-PET showed better specificity than bone scans [14].

Moog et al. studied 56 patients in primary staging of malignant lymphoma, (34 Hodgkin's disease, 22 NHL) [15]. Both imaging techniques revealed positive concordant imaging findings in 12/56 of them, although  $^{18}\text{F}$ FDG-PET was superior to skeletal scintigraphy in detecting bone marrow infiltration in 30 regions and whereas skeletal scintigraphy only revealed bone marrow infiltration in 20 regions. These findings were confirmed by biopsy, CT, MRI and skeletal scintigraphy. Moog et al. found that  $^{18}\text{F}$ FDG-PET is suitable for identifying osseous involvement in malignant lymphoma and that it is more sensitive and specific than bone scintigraphy [15]. However, they did not directly compare  $^{18}\text{F}$ FDG-PET to MRI in the assessment of bone and bone marrow lesions. Ghanem et al. carried out a retrospective examination of 38 patients, noting eight discordant findings between MRI and  $^{18}\text{F}$ FDG-PET in the spine [13]. In seven of their eight cases, the  $^{18}\text{F}$ FDG-PET was false negative and a therapeutic measure was carried out in two of the seven cases. In one case the  $^{18}\text{F}$ FDG-PET finding were false positive [13].

False-positive  $^{18}\text{F}$ FDG-PET results are caused by sacral fractures [9]. Fayad et al. studied three patients with colorectal cancer who had insufficiency fractures; however, cross-sectional CT or MRI imaging can differentiate the

FDG-uptake caused by fractures and the FDG-accumulation due to tumoural infiltration [9].

In addition to skeletal scintigraphy, PET is an imaging modality increasingly being used to successfully diagnose skeletal metastases. In the latter method, the radiotracer  $^{18}\text{F}$ fluoride is used in addition to  $^{18}\text{F}$ -FDG [17]. However,  $^{18}\text{F}$ FDG-PET was not primarily indicated solely for the assessment of bone metastases. In cases when  $^{18}\text{F}$ -FDG-PET was carried out, the additional findings of bone metastases were made via the non-specific phenomenon of increased glycolysis in malignant cells [6].

Few studies exist which compare  $^{18}\text{F}$ -fluoride-PET with MRI. Schirrmester et al. [17] compared  $^{18}\text{F}$ -fluoride-PET with skeletal scintigraphy, whereby  $^{18}\text{F}$ -fluoride-PET detected 64 skeletal metastases in 17 of the 34 patients [17]. Skeletal scintigraphy findings, positive in only 11 of the 34 patients, detected 29 metastases. Some authors suggest that  $^{18}\text{F}$ FDG-PET will eventually replace skeletal scintigraphy [6]. Schirrmester et al. [17] compared  $^{18}\text{F}$ -fluoride-PET with SPECT and planar skeletal scintigraphy in breast and lung cancer patients and showed the definite superiority of  $^{18}\text{F}$ -fluoride-PET to planar skeletal scintigraphy with and without the incorporation of the SPECT technique [17].

So finally, the heterogeneity of our patient population might create a certain bias in our direct comparison. We included fast and slow growing tumours in our retrospective study, leading to a certain tendency. Further prospective studies with a selected patient group are necessary.

In conclusion, we observed MRI to be superior to  $^{18}\text{F}$ FDG-PET in detecting bone marrow metastases and marrow infiltration of the spine in patients with solid tumours and lymphoma. MRI reveals important additional information such as like pathological fractures, spinal canal involvement and intraspinal and medullary metastases, having therapeutic consequences. MRI is more sensitive and specific in visualising bone marrow metastasis and infiltration of the spine. In cases of false positive PET scans, MRI of the spine depicts no bone marrow infiltration. In cancer patients with bone pain and neurological symptoms, and in cases of a negative  $^{18}\text{F}$ FDG-PET-scan MRI of the spine should be performed to document actual and potential complications of bone marrow metastasis or infiltration.

## References

- Abrams HL, Spiro R, Goldstein N (1950) Metastases in carcinoma: analysis of 1000 autopsied cases. *Cancer* 3:336–340
- Altehoefer C, Blum U, Bathmann J, Wüstenberg C, Uhrmeister P, Laubenberger J, Lange W, Schwarzkopf J, Moser E, Langer M (1997) Comparative accuracy of magnetic resonance imaging and immunoscintigraphy for detection of bone marrow involvement in patients with malignant lymphoma. *J Clin Oncol* 15:1754–1760
- Altehoefer C, Ghanem N, Högerle S, Moser E, Langer M (2001) Comparative detectability of bone metastases and impact on therapy of magnetic resonance imaging and bone marrow scintigraphy in patients with breast cancer. *Eur J Radiol* 40:16–23
- Baur A, Stäbler A, Nagel D et al (2002) Magnetic resonance imaging as a supplement for clinical staging system of Durie and Salmon? *Cancer* 95:1334–45
- Bares R (1998) Skeletal scintigraphy in breast cancer management. *Q J Nucl Med* 42:43–48
- Brink I, Schumacher T, Mix M et al (2004) FDG-PET on the primary staging of small-cell lung cancer. *Eur J Nucl Med Mol Imaging* 31:1614–1620
- Cook GJ, Houston S, Rubens RD, Maisey MN, Fogelman I (1998) Detection of bone metastases in breast cancer by  $^{18}\text{F}$ FDG PET: differing metabolic activity in osteoblastic and osteolytic lesions. *J Clin Oncol* 16:3375–3379
- Daldrup-Link HE, Franzius C, Link TM, Laukamp D, Sciuk J, Jurgens H, Schober O, Rummeny EJ (2001) Whole-body MR imaging for detection of bone metastases in children and young adults: comparison with skeletal scintigraphy and FDG-PET. *AJR Am J Roentgenol* 177:229–236
- Fayad LM, Cohade C, Wahl RW, Fishman EK (2003) Sacral fractures: a potential pitfall of FDG-PET. *AJR Am J Roentgenol* 181:1239–1243
- Franzius C, Daldrup-Link HE, Wagner-Bohn A, Sciuk J, Heindel WL, Jürgens H, Schober O (2002) FDG-PET for detection of recurrences from malignant primary bone tumors and comparison with conventional imaging. *Ann Oncol* 13:157–160
- Franzius C, Sciuk J, Daldrup-Link HE, Jurgens H, Schober O (2000) FDG-PET for detection of osseous metastases from malignant primary bone tumours: comparison with bone scintigraphy. *Eur J Nucl Med* 27:1305–1311
- Ghanem N, Altehoefer C, Högerle S et al (2002) MRI and FDG-PET of the axial skeleton in cancer patients. *ESSR 2002, IX Annual Meeting*. pp 191–192
- Ghanem N, Altehoefer C, Högerle S, Schäfer O, Winterer J, Moser E, Langer M (2002) Comparative diagnostic value and therapeutic relevance of magnetic resonance imaging and bone marrow scintigraphy in patients with metastatic solid tumors of the axial skeleton. *Eur J Radiol* 43:256–261
- Kao CH, Hsieh JF, Tsai SC, Ho YJ, Yen RF (2000) Comparison and discrepancy of  $^{18}\text{F}$ -2-deoxyglucose positron emission tomography and Tc-99m MDP bone scan to detect bone metastases. *Anticancer Res* 20:2189–2192
- Moog F, Kotzerke J, Reske SN (1999) FDG PET can replace bone scintigraphy in primary staging of malignant lymphoma. *J Nucl Med* 40:1407–1413
- Munker R, Hasenclever D, Brosteanu O et al (1995) Bone marrow involvement in Hodgkin's disease: an analysis of 135 consecutive cases. *J Clin Oncol* 13:403–409
- Schirrmester H, Guhlmann A, Kotzerke J et al (1999) Early detection and accurate description of extent of metastatic bone disease in breast cancer with fluoride ion and positron emission tomography. *J Clin Oncol* 17:2381–2389
- Sherry MM, Greco FA, Johnson DH, Hainsworth ID (1986) Breast cancer with skeletal metastases at initial diagnosis. Distinctive clinical characteristics and favourable prognosis. *Cancer* 58:178–182
- Shreve PD, Barton GH, Gross MD, Wahl RL (1996) Metastatic prostate cancer: Initial findings of PET with 2-Deoxy-2-( $^{18}\text{F}$ )fluoro-d<sup>1</sup>-glucose. *Radiology* 199:751–756
- Wikenheiser KA, Silberstein EB (1996) Bone scintigraphy screening in stage I-II breast cancer: Is it cost-effective? *Cleveland Clin J Med* 63:43–44